Clim. Past Discuss., 4, 1089–1113, 2008
www.clim-past-discuss.net/4/1089/2008/


Climate of the Past Discussions

*Climate of the Past Discussions* is the access reviewed discussion forum of *Climate of the Past*



# Two millennia of climate variability in the Central Mediterranean

**C. Taricco[1,2], M. Ghil[3,4], and G. Vivaldo[1,2]**

[1]Dipartimento di Fisica Generale, University of Torino, Torino, Italy
[2]Istituto di Fisica dello Spazio Interplanetario-INAF, University of Torino, Torino, Italy
[3]Département Terre-Atmosphère-Océan & Laboratoire de Météorologie Dynamique (CNRS and IPSL), Ecole Normale Supérieure, Paris, France
[4]Department of Atmospheric and Oceanic Sciences, Institute of Geophysics and Planetary Physics, University of California, Los Angeles, CA, USA

Received: 14 July 2008 – Accepted: 14 July 2008 – Published: 1 October 2008

Correspondence to: C. Taricco (taricco@ph.unito.it)

Published by Copernicus Publications on behalf of the European Geosciences Union.

## Abstract

This experimental work addresses the need for high-resolution, long and homogeneous climatic time series that facilitate the study of climate variability over time scales of decades to millennia. We present a high-resolution record of foraminiferal $\delta^{18}$O from a Central Mediterranean sediment core that covers the last two millennia. The record was analyzed using advanced spectral methods and shows highly significant oscillatory components with periods of roughly 600, 350, 200, 125 and 11 years. Comparison with the spectra of composite temperature-proxy series over the last millennium reveals that the $\delta^{18}$O trend and 200-y components are well correlated with the long-term Northern Hemisphere temperature variations over the last millennium, showing a maximum at the Medieval Optimum and a shallower local minimum at the Little Ice Age. In the preceding millennium the same $\delta^{18}$O components also reveal a deep maximum (temperature minimum) at about 0 AD.

## 1 Introduction

Knowledge of long-term natural variability is required to assess anthropogenic effects on climate (Martinson et al., 1995; National Research Council, 2006). Instrumental temperature series, however, cover only a couple of centuries (Ghil and Vautard, 1991; Martinson et al., 1995; Plaut et al., 1995; Jones et al., 1999; Folland and Karl, 2001; National Research Council, 2006); therefore, in order to estimate climatic variations over the last millennium, several temperature series have been constructed, using single-proxy, such as tree rings (Luckman et al., 1997; Esper et al., 2002), or multi-proxy records (Jones et al., 1998; Mann et al., 1999; Crowley, 2000). Multi-proxy records extend the spatial coverage of climate reconstructions, typically using ice cores (Jones, 1996) for high latitudes, tree rings (Luckman et al., 1997; Esper et al., 2002) for mid-latitudes, and corals (Crowley, 2000; Boiseau et al., 1999) for low latitudes. Each of these proxies, however, reflects a different combination of temperature and precipitation effects and thus the interpolation and averaging over multi-proxy records (Jones et al., 1998; Mann et al., 1999; Crowley, 2000) may lead to spurious variations in the reconstructions (Jones, 1996; Esper et al., 2004; Von Storch et al., 2004).

Marine cores with very high sedimentation rates allow one to investigate climate variations on scales of decades to millennia. They may also reflect broader features of climate, since the circulation of the basin in which they are located produces at least regional averaging (Martinson et al., 1995). In order to avoid possible artifacts produced by the composition of different proxies, we have measured the oxygen isotope composition $\delta^{18}O$ of planktonic foraminifera in a high-resolution, well-dated Central Mediterranean core. These measurements yield a homogeneous, 2200-year-long record, which captures climatic oscillations with a broad range of periods, from decades to centuries. We compare our series with other climate records, to gain information about long-term climate variations in the Northern Hemisphere (NH).

## 2 Experimental procedure

Over the last 20 years, the Torino cosmogeophysics group has carried out the absolute dating of shallow-water Ionian Sea cores, drilled from the Gallipoli Terrace in the Gulf of Taranto (Fig. 1). This carbonatic mud deposit is located at about 200 m of water depth. The high accuracy of the dating is made possible by the closeness of the drilling site to the volcanic Campanian area, a region that is unique in the world by its detailed historical documentation of volcanic eruptions over the last two millennia. The markers of these eruptions were identified along the cores as peaks of the number density of clinopyroxene crystals, carried by the prevailing westerly winds from their source into the Ionian Sea and deposited there as part of its marine sediments. The time-depth relation for the cores retrieved from the Gallipoli Terrace (Bonino et al., 1993; Cini Castagnoli et al., 1990, 1992a, 1999, 2002a) was obtained by tephroanalysis; this analysis confirmed, improved and extended to the deeper part of the core the dating obtained in the upper 20 cm by the $^{210}Pb$ method (Krishnaswamy et al., 1971; Bonino et al., 1993). The dating previously obtained has been recently confirmed (Taricco et al., 2008) by applying advanced statistical procedures (Guo et al., 1999; Naveau et al., 2003).

The cores were sampled every 2.5 mm and the number density of clinopyroxenes of clear volcanic origin, characterized by skeletal morphology and sector zoning, was determined for the portion of the cores that covers the last two millennia. We found 22 sharp pyroxene peaks, corresponding to the historical eruptions of the Campanian area, starting with the 79 AD eruption of the Vesuvius that buried Pompei and ending with its last eruption in 1944 (Arnò et al., 1987).

Figure 2 shows the time-depth relation over the last two millennia. Each point represents a pyroxene peak found at a given depth, corresponding to a historical eruption. The linear regression gives $h=(0.0645\pm0.0002)y_{BT}$, where $h$ is depth in cm, $y_{BT}$ means year-before-top (top = 1979 AD) and the correlation coefficient is $r=0.99$; the slope of this line is the sedimentation rate. This relatively high sedimentation rate allows high-resolution studies in time: the sampling interval of the core, 2.5 mm, corresponds in fact to 3.87 y. The highly linear time-depth relation demonstrates that the sedimentation rate has remained constant, to a very good approximation, over the last two millennia. Moreover, the measurements performed in different cores retrieved from the same area showed that this rate is also uniform across the whole Gallipoli Terrace (Cini Castagnoli et al., 1990, 1992a, 2002a,b). The very sharp pyroxene peaks indicate that bioturbation by bottom-dwelling organisms is quite limited; we thus conclude that the climatic record is not significantly affected by sediment mixing.

## 3 Results

In Fig. 3 we present the $\delta^{18}$O measurements of the surface-dwelling foraminifera *Globigerinoides ruber* in the 3.57 m-long core GT90/3 (39°45′53″ N, 17°53′33″ E). Stable-isotope analysis has been completed for the upper 140 cm of this core, as discussed in Appendix A.



CPD

4, 1089–1113, 2008

The $\delta^{18}O$ profile consists of a continuous record of 560 points from 200 BC to 1979 AD, with a sampling interval of $\Delta t = 3.87$ y. We analyzed this series by several spectral methods, including classical Fourier analysis, the maximum entropy method (MEM), and singular-spectrum analysis (SSA). The typical problem of classical spectral estimates, besides power leakage and high variance, is the use of a fixed basis of harmonic functions (sines and cosines). In contrast, SSA uses data-adaptive basis functions; this feature makes the method particularly useful for climatic time series (Vautard et al., 1992), which are most often short and noisy. The SSA methodology (see Appendix B1) has in fact been applied to many instrumental and proxy climate records (e.g., Ghil and Vautard, 1991; Plaut et al., 1995; Cini Castagnoli et al., 2002a); two review papers (Ghil and Taricco, 1997; Ghil et al., 2002) and references therein cover the methodology as well as numerous other applications. We used the SSA-MTM Toolkit (see Ghil et al., 2002, and the freeware toolkit at http://www.atmos.ucla.edu/tcd/ssa/) and focus here on the results obtained by SSA. These results were confirmed by other methods, such as MTM (not shown).

We adopted a window width of $M = 150$ points, corresponding to a time window of $M\Delta t \simeq 580$ y, in order to be able to detect oscillations with a period as long as 500–600 y, while maintaining sufficient statistical significance. We obtained very similar results for a fairly wide range of $M$ values, from 120 to 200 points.

The empirical orthogonal functions (EOFs) 1–12 account for roughly 42% of the total variance in the $\delta^{18}O$ time series. Monte Carlo-SSA (Allen and Smith, 1996; see also Appendix B2) allows us to verify that the statistically significant part of the $\delta^{18}O$ time series is given by the sum of these 12 components, with a residue of red noise; RCs 1–8 and 11-12 are significant at the 99% confidence level, and RCs 9–10 at the 98% level.

Figure 4 shows the spectral properties of our proxy record. The error bars plotted in the main panel of Fig. 4 bracket 99% of the eigenvalues obtained by the SSA of 10 000 surrogate series; these series are generated by a model that superposes EOFs 1–12 onto a red-noise process, i.e. an auto-regressive process of order 1, or AR(1). The eigenvalues that lie outside the 99% error bars are only those associated with EOFs 1–12, which have been included in the null hypothesis; this confirms that the model AR(1)+EOFs 1–12 captures the $\delta^{18}$O time series, at the 99% confidence level. We obtained this result after having rejected, at the same confidence level, a whole range of null hypotheses, including different combinations of EOFs.

EOF-1 corresponds to the nonlinear, data-adaptive trend of the series, while the EOF pairs 2–3, 4–5, 9–10 and 11–12, and the EOF "triplet" 6–8 (Vautard et al., 1992) capture oscillatory components; the periods associated with these components were determined by MEM applied to each component separately. The periods so obtained (and corresponding variances) equal 595 y (14.1%), 352 y (6.7%), 190 y (4.8%), 125 y (2.4%) and 11.4 y (2.3%); see the MEM spectrum in the inset of Fig. 4.

The trend RC-1 (see Fig. 5a) exhibits a pronounced maximum near 0 AD, as well as a pronounced minimum at the Medieval Optimum (MO: 1000–1200 AD); the reconstruction (Ghil and Vautard, 1991; Ghil and Taricco, 1997; Ghil et al., 2002) of the $\delta^{18}$O series, using RCs 1–12, is shown in Fig. 3, superposed on the raw data.

We compared the statistically significant $\delta^{18}$O components of our record with several NH temperature series over the last 1000 y (Luckman et al., 1997; Jones et al., 1998; Mann et al., 1999; Crowley, 2000; Esper et al., 2002, 2004). This comparison should clarify first the extent to which our $\delta^{18}$O record is temperature dominated, and second to which extent it is representative of hemispheric climate variability on the time scales of interest. This set of references provides a fairly comprehensive view of variability over the past millennium (National Research Council, 2006), while the longer time series of Mann and Jones (2003) is based merely on a very few and unevenly distributed indicators, and thus represents a more tentative view of NH climate variability over the previous millennium.

We performed first the SSA analysis of the annually resolved time series of Mann et al. (1999), using a window of $M$=300 points, i.e., $M\Delta t$=300 y. The leading RCs 1–4 capture about 70% of the variance associated with the significant components of the series. These RCs represent a trend (RCs 1, 4), shown in Fig. 5a (red line), and a 200-y oscillation (RCs 2–3), shown in Fig. 5b (red line); both are significant at the 99% confidence level. These components together describe well the long-term NH temperature variation in the last millennium (see red line in Fig. 6, superposed on the original temperature series of Mann et al., 1999).

In Fig. 5 we show also the corresponding signals contained in our record: the trend (RC-1) in panel (a) and the 200-y oscillation (RCs 6–8) in panel (b) (black lines). Over the last millennium, the match between these two $\delta^{18}$O signals and the corresponding ones in the Mann et al. (1999) NH temperature proxy record is excellent. Therefore, over the last 1000 years we consider the sum $\Sigma$ of the trend and 200-y components in the $\delta^{18}$O series as representative of the long-term NH temperature variability (see black line in Fig. 6, in fair agreement with the Mann red line in the same figure). In fact $\Sigma(t)$, where $t=1979-y_{BT}$ is time (expressed in years BC or AD), describes the temperature decrease from the Medieval Warm Period (MWP) to the Little Ice Age (LIA), as well as the temperature minima around 1500, 1700 and 1900 AD, depicted by the 200-y cycle and often associated with the Spörer (~1500 AD), Maunder (~1700 AD) and Modern (~1900 AD) minima of solar activity. Moreover the temperature increase during the industrial era (IE) is evident.

The linear regression between the black and red curves in Fig. 6 gives

$$T = -(0.102 \pm 0.005) - (1.62 \pm 0.08)\Sigma, \tag{1}$$

with $\Sigma$ in ‰ and $T$ in °C; the correlation coefficient between $T$ and the right-hand side of the equation is $r=-0.8$. This high correlation allows us to calibrate the black curve in terms of NH temperature, with 1 corresponding to 1.6°C; NH temperature variations are thus given by $\Delta T_{NH} \simeq -1.6\ \Delta\Sigma$.

The trend present in the proxy record of Jones et al. (1998) (see Fig. 5a) agrees well with that of Mann et al. (1999). Moreover, the 200-y oscillation is present at a 99% confidence level in each of the reconstructed temperature series of reference (Luckman et al., 1997; Jones et al., 1998; Mann et al., 1999; Crowley, 2000; Esper et al., 2002; not shown in Fig. 5b). The 300-y oscillation appears as RCs 4–5 in our $\delta^{18}$O record and is the dominant component of the Jasper tree-ring time series (Luckman et al., 1997), where it appears as RCs 1–2 (not shown), but it is not present in other proxy records (Esper et al., 2004).

Stuiver and Braziunas (1993) found a 500-y oscillation to dominate the spectrum of $\Delta^{14}$C over the last 12 ky, and related it to salinity changes associated with an oscillation of the oceans' thermohaline circulation (Stommel, 1961; Bryan et al., 1986; Tzipermann, 1997; Ghil , 2001). In the 1200-y, tree-ring based NH temperature reconstruction of Esper et al. (2002), a 500-y oscillation also dominates: it is captured by RCs 1–2 (with $M\Delta t$=500 y) and is in phase with RCs 2–3 of our $\delta^{18}$O record. This feature, as well as the 300-y oscillation of Esper et al. (2002), is not present in other proxy temperature records (Esper et al., 2004) and therefore we did not include them in the multi-centennial temperature reconstruction $\Sigma$ of Fig. 6.

Due to the high resolution of the $\delta^{18}$O series, we capture also an 11.4-y component (RCs 11–12) with a 99% confidence level. Cini Castagnoli et al. (1999) showed that the 11-y cycle in the $\delta^{18}$O of core GT90/3 is perfectly in phase with the solar cycle. The average amplitude of this cycle is $\sim$0.04‰ over 2200 y. White et al. (1997) found an 11-y cycle in global sea-surface temperatures (SSTs) over the last century and attributed its small amplitude of $0.04\pm0.01^{\circ}$C to the direct response of the upper ocean to changing solar irradiance. If we apply the tentative $\Sigma$–$T$ calibration found before, i.e. $\Delta T_{NH}\simeq-1.6\ \Delta\Sigma$, we obtain an average amplitude of $\sim1.6\times0.04=0.06^{\circ}$C for the NH. This last value is in reasonable agreement with White et al. (1997).

## 4 Discussion

The sum $\Sigma(t)$ of the two $\delta^{18}$O components (trend and 200-y oscillation), which describes well the NH temperature variations in the last millennium, is shown in Fig. 6 also for the preceding millennium (black curve), where only limited and less accurate information is available. During this time interval, the 200-y oscillation still exhibits pronounced temperature minima (i.e., $\delta^{18}$O maxima), e.g. at 450 AD and 650 AD.

The most striking feature of Fig. 6 is the steep $\delta^{18}$O decrease of ∼0.23‰ from 0 AD to the MO (∼1100 AD), indicating considerably colder temperatures around 0 AD. Most $\delta^{18}$O variations observed in $\Sigma(t)$ over the last 2 millennia can be correlated and are in phase with known climate oscillations, such as the Dark Ages (DA), the MWP and the LIA; the low temperatures reconstructed around 0 AD, however, are in disagreement with the relative warmth often attributed to the "Roman Classical Period" (RCP). Evidence for and against high temperatures during the RCP is discussed in the following paragraphs.

Temperature profiles in the GRIP and Dye-3 ice cores indicate cold temperatures, though higher than during the LIA (Dahl-Jensen et al., 1998, see Fig. 7 here, first panel). Bond et al. (2001) show that around 0 AD the temperatures in high northern latitudes were comparable to those during the LIA. The reconstruction indicating the lowest temperatures for the period around 0 AD is the one of DeMenocal et al. (2000; see Fig. 7 here, third panel), who reported very low sea surface temperatures (SSTs) off western Africa at about 2000 y BP. Moreover a peat bog record analyzed by Martínez-Cortizas et al. (1999) indicates a local minimum around 2000 BP, followed by a long warm period. A study of wood buried in the Roman siege ramp of the Masada fortress near the Dead Sea suggests a cold and wet period around 70 AD (Issar and Yakir, 1997).

The SST profile at the Bermuda Rise measured by Keigwin (1996; see Fig. 7 here, second panel) shows a temperature decrease between 200 BC and 200 AD and therefore a temperature minumum that is somewhat delayed with respect to the above-mentioned references.

In contrast to these arguments in favor of cool conditions around 0 AD, there are other proxy records that point instead to relatively high temperatures. A recent high-resolution record from the Atlantic off North Iceland (Sicre et al., 2008) reports SSTs between 0 and 100 AD that are similar to those observed during the MWP.

Several proxies of glacier retreat (Holzauser et al., 2005; Joerin et al., 2006) and of low lake levels on the Swiss plateau (Holzauser et al., 2005) indicate warm and/or dry conditions in the Alps during the RCP. A recent review (Reale and Dirmeyer, 2000) of Mediterranean climate history indicates a gradual drying and warming between the Greek Classical Period (5th century BC) and the Late Roman Period (5th century AD). This warming trend continued until 900 AD, followed by relatively high temperatures between 900 and 1300 AD.

A general circulation model simulation by Reale and Shukla (2000) suggests possibly dry conditions over the Mediterranean itself, due to the changes in atmospheric circulation. A prominent positive peak of about 0.5‰ in $\delta^{18}O$ is also seen in the Eastern Mediterranean record of Schilman et al. (2001), who interpreted this peak as an indication of increased aridity in the Eastern Mediterranean. If the entire 0.5‰ change is attributed to salinity changes, then the $\delta^{18}O$ – salinity relationship of Pierre (1999) would yield roughly a salinity change of up to 2 PSU. Such a high salinity increase is fairly unlikely, thus suggesting that the $\delta^{18}O$ variation of Schilman and co-authors is due at least in part to a temperature decrease.

Across this contradictory evidence about temperatures during the RCP, general agreement is found regarding a decrease of precipitations in the Mediterranean area during this period, possibly explaining the reduction of the glacial extent and lake levels in the Alps. This decrease in precipitations could have reduced the freshwater inflow into the Adriatic Sea, especially through the Po River. As a consequence, the salinity and hence the $\delta^{18}O$ of the Adriatic waters flowing into the Gulf of Taranto might have increased. This isotopic change of the water, together with somewhat lower temperatures, could have contributed to the high $\delta^{18}O$ values measured in our core at the beginning of the Current Era.

## 5 Conclusions

A 2200-year-long, high-resolution record of foraminineral $\delta^{18}O$ from a sediment core drilled in the Gulf of Taranto was measured and studied. The time series analysis, carried out with advanced spectral methods, reveals the presence of highly significant oscillatory components with periods of roughly 600, 350, 200, 125 and 11 y. The comparison with Northern Hemisphere (NH) temperature series previously reconstructed over the last 1000 y indicates that the $\delta^{18}$O trend and 200-y components are temperature-driven and that together they describe well the long-term NH temperature variability over the last millennium. Moreover, a maximum at the Medieval Optimum and a much shallower local minimum at the Little Ice Age are detected.

In the preceding millennium, the same two components describe a long-lasting interval of high $\delta^{18}$O and presumably low temperatures, which coincides in part with the Roman Classical Period (RCP) and thus contradicts the commonly alleged warmth of this period. While broadly accepted effects of drier climate and hence higher salinity may explain at least part of this $\delta^{18}$O maximum, one needs additional proxy-record analyses in order to disentangle the temperature and salinity effects, and to better justify the use of the trend and 200-y components in the first millennium to reconstruct temperature variations.

Finally, we emphasize that the absolute dating of our Gulf of Taranto cores, based on a reliable sample of historically documented volcanic markers over the last two millennia, ensures an uncommon reliability in the timing of the climate proxies we analyzed.

## Appendix A

### Stable isotope analysis

In order to obtain the $\delta^{18}$O value of the samples, taken with a spacing of 2.5 mm, we soaked 5 g of sediment in 5% calgon solution overnight, then treated it in 10% $H_2O_2$ to remove any residual organic material, and subsequently washed it with a distilled-water jet through a sieve with a 150 $\mu$m mesh. The fraction >150 $\mu$m was kept and oven-dried at 50°C. The planktonic foraminifera *Globigerinoides ruber* were picked out of the samples under the microscope. For each sample, 20–30 specimens were selected from the fraction comprised between 150 $\mu$m and 300 $\mu$m.

The use of a relatively large number of specimens for each sample removes the isotopic variability of the individual organisms, giving a more representative $\delta^{18}O$ value. The stable isotope measurements were performed using a VG-PRISM mass spectrometer fitted with an automated ISOCARB preparation device. Analytical precision based on internal standards was better than 0.1‰. Calibration of the mass spectrometer to VPDB scale was done using NBS19 and NBS18 carbonate standards.

## Appendix B

### B1 Singular Spectrum Analysis (SSA)

The SSA methodology involves three basic steps: (1) embedding a time series of length $N$ in a vector space of dimension $M$ (for the choice of $M$, see Vautard et al., 1992; Ghil et al., 2002); (2) computing the $M \times M$ lag-covariance matrix $\mathbf{C}_D$ of the data (see the two different approaches of Broomhead et al., 1986, and Vautard and Ghil, 1989); and (3) diagonalizing $\mathbf{C}_D$:

$$\mathbf{\Lambda}_D = \mathbf{E}_D^T \mathbf{C}_D \mathbf{E}_D,$$

where $\mathbf{\Lambda}_D$=diag$(\lambda_1, \lambda_2, \ldots \lambda_M)$, with $\lambda_1, \lambda_2, \ldots \lambda_M \geq 0$, and $\mathbf{E}_D$ is the $M \times M$ matrix having the corresponding eigenvectors $\boldsymbol{E}_k$, $k=1, \ldots, M$ as its columns. For each $\boldsymbol{E}_k$ we construct the time series, of length $N-M+1$, called the $k$-th principal component (PC); this PC represents the projection of the original time series on the eigenvector $\boldsymbol{E}_k$ (also called empirical orthogonal function, EOF). Each eigenvalue $\lambda_k$ gives the variance of the corresponding PC; its square root is called singular value (SV). Given a subset of eigenvalues, it is possible to extract time series of length $N$, by combining the corresponding PCs; these time series are called reconstructed components (RCs) and capture the variability associated with the eigenvalues of interest.

## B2 Monte Carlo SSA (MC-SSA)

In order to reliably identify the trend and oscillations of the $\delta^{18}O$ time series, we used the Monte Carlo method (MC-SSA) (Allen and Smith, 1996). In this approach, we assume a model for the analysed time series (null-hypothesis) and we determine the parameters using a maximum-likelihood criterion. Then a Monte Carlo ensemble of surrogate time series (size 10 000) is generated from the model and SSA is applied to data and surrogates (EOFs of the null-hypothesis basis are used), in order to test whether it is possible to distinguish the series from the ensemble. Since a large class of geophysical processes generates series with larger power at lower frequencies, we have assumed AR(1) noise in evaluating evidence for trend and oscillations. This is done to avoid overestimating the system's predictability, by underestimating the amplitude of the stochastic component of the time series (Allen and Smith, 1996).

*Acknowledgements.* It is a pleasure to honor by this paper the lifelong contributions of André Berger, a close friend of one of the authors (M.G.): having contributed substantially to the understanding of the link between secular changes in the planetary orbits and glaciation cycles on Earth, André Berger turned his attention to the recent past and the future of Earth's climate.

We also wish to recall the memory of Giuliana Cini Castagnoli, who lead the Cosmogeophysics Group at Torino for many years, and of Giuseppe Bonino, who contributed significantly to this study. We are grateful to the late Carlo Castagnoli for stimulating discussions and support.

We wish to thank S. M. Bernasconi (Geological Institute, ETH, Zürich, Switzerland) for the mass spectrometer measurements of our samples, for having drawn our attention to several papers on climatic proxy records, and for several interesting discussions, J. C. Duplessy and S. Alessio for their constructive comments, and A. Romero for his dedicated technical assistance.

This collaborative research was supported by the European Commission's Project No. 12975 (NEST) "Extreme events: Causes and consequences (E2-C2)". MG's work was also partially supported by US Department of Energy grant DE-FG02-07ER64439 from its Climate Change Prediction Program.

## References

Allen, M. R. and Smith, L. A.: Monte Carlo SSA: detecting oscillations in the presence of coloured noise, J. Climate, 9, 3373–3404, 1996. 1093, 1101, 1110

Arnò, V., Principe, C., Rosi, M., Santacroce, R., Sbrana, A., and Sheridan, M. F.: Eruptive History, in: Summa-Vesuvius, Quaderni de La Ricerca Scientifica, edited by: Santacroce R., CNR, Roma, Italy, 114(8), 53–103, 1987. 1092

Boiseau, M., Ghil, M., and Juillet-Leclerc, A.: Climatic trends and interdecadal variability from South-Central Pacific coral records, Geophys. Res. Lett., 26, 2881–2884, 1999. 1090

Bond, G., Kromer, B., Beer, J., Muscheler, R., Evans, M. N., Showers, W., Hoffmann, S., Lotti-Bond, R., Hajdas, I., and Bonani, G.: Persistent solar influence on North Atlantic climate during the Holocene, Science, 294(5549), 2130–2136, 2001. 1097

Bonino, G., Cini Castagnoli, G., Callegari, E., and Zhu, G. M.: Radiometric and tephroanalysis dating of recent Ionian sea cores, Nuovo Cimento C, 16, 155–161, 1993. 1091, 1107

Broomhead, D. S. and King, G. P.: Extracting qualitative dynamics from experimental data, Physica D, 20, 217–236, 1986. 1100

Brian, F.: High-latitude salinity effects and interhemispheric thermohaline circulations, Nature, 323, 301–304, 1986. 1096

Cini Castagnoli, G., Bonino, G., Caprioglio, F., Provenzale, A., Serio, M., and Zhu, G. M.: The carbonate profile of two recent Ionian sea cores: evidence that the sedimentation rate is constant over the last millenia, Geophys. Res. Lett., 17, 1937–1940, 1990. 1091, 1092, 1107

Cini Castagnoli, G., Bonino, G., Provenzale, A., Serio, M., and Callegari, E.: The $CaCO_3$ profiles of deep and shallow Mediterranean sea cores as indicators of past solar-terrestrial relationship, Nuovo Cimento C, 15, 547–563, 1992a. 1091, 1092, 1107

Cini Castagnoli, G., Bonino, G., Serio, M., and Sonett, C. P.: Common spectral features in the 5500-year record of total carbonate in sea sediments and radiocarbon in tree rings, Radiocarbon, 34(3), 798–805, 1992b. 1107

Cini Castagnoli, G., Bonino, G., Della Monica, P., and Taricco, C.: Record of thermoluminescence in sea sediments in the last millennia, Nuovo Cimento C, 20(1), 1–8, 1997. 1107

Cini Castagnoli, G., Bonino, G., and Taricco, C.: The global and persistent millennial-scale variability in the thermoluminescence profiles of shallow and deep Mediterranean sea cores, Nuovo Cimento C, 21, 453–460, 1998. 1107

Cini Castagnoli, G., Bonino, G., Della Monica, P., Taricco, C., and Bernasconi, S. M.: Solar activity in the last millennium recorded in the $\delta^{18}$O profile of planktonic foraminifera of a shallow water Ionian Sea core, Sol. Phys., 188(1), 191–202, 1999. 1091, 1096, 1107

Cini Castagnoli, G., Bonino, G., and Taricco, C.: Long term solar-terrestrial records from sediments: carbon isotopes in planktonic foraminifera during the last millennium, Adv. Space Res., 29(10), 1537–1549, 2002a. 1091, 1092, 1093

Cini Castagnoli, G., Bonino, G., Taricco, C., and Bernasconi S. M.: Solar radiation variability in the last 1400 years recorded in the carbon isotope ratio of a mediterranean sea core, Adv. Space Res., 29(12), 1987–1994, 2002b. 1092, 1107

Cini Castagnoli, G., Taricco, C., and Alessio, S.: Isotopic record in a marine shallow-water core: imprint of solar centennial cycles in the past 2 millennia, Adv. Space Res., 35, 504–508, 2005. 1107

Crowley, T. J.: Causes of climate change over the past 1000 years, Science, 289(5477), 270–277, 2000. 1090, 1091, 1094, 1095

DeMenocal, P., Ortiz, J., Guilderson, T., and Sarnthein, M.: Coherent high- and low-latitude climate variability during the Holocene Warm Period, Science, 288, 2198–2202, 2000. 1097, 1113

Dahl-Jensen, D., Mosegaard, K., Gundestrup, N., Clow, G. D., Johnsen, S. J., Hansen, A. W., and Balling, N.: Past temperatures directly from the Greenland ice sheet, Science, 282, 268–271, 1998. 1097, 1113

Esper, J., Cook, E. R., ans Schweingruber, F. H.: Low-frequency signals in long tree-ring chronologies and the reconstruction of past temperature variability, Science, 295(5563), 2250–2253, 2002. 1090, 1094, 1095, 1096

Esper, J., Frank, D. C., and Wilson, R. J. S.: Climate reconstructions – low frequency ambition and high frequency ratification, Eos Trans. AGU, 85(12), 113–120, 2004. 1091, 1094, 1096

Folland, C. K. and Karl, T. L.: Recent rates of warming in marine environment meet controversy, Eos Trans. AGU, 82(40), 453–459, 2001. 1090

Ghil, M.: Hilbert problems for the geosciences in the 21st century M., Nonlin. Processes Geophys., 8, 211–222, 2001, http://www.nonlin-processes-geophys.net/8/211/2001/. 1096

Ghil, M. and Taricco, C.: Advanced spectral analysis methods, in: Past and Present Variability of the Solar-terrestrial System: Measurement, Data Analysis and Theoretical Models, edited by: Cini Castagnoli, G. and Provenzale, A., IOS Press, Amsterdam, The Netherlands, 137–

159, 1997. 1093, 1094, 1109

Ghil, M. and Vautard, R.: Interdecadal oscillations and the warming trend in global temperature time series, Nature, 350, 324–327, 1991. 1090, 1093, 1094, 1109

Ghil, M., Allen, M. R., Dettinger, M. D., Ide, K., Kondrashov, D., Mann, M. E., Robertson, A. W., Saunders, A., Tian, Y., Varadi, F., and Yiou, P.: Advanced spectral methods for climatic time series, Rev. Geophys., 40(1), 3.1–3.41, 2002. 1093, 1094, 1100, 1109

Guo, W., Wang, Y., and Brown, M. B.: A signal extraction approach to modelling hormone time series with pulses and a changing baseline, J. Am. Stat. Assoc., 94(447), 746–756, 1999. 1092

Holzhauser, H., Magny, M., and Zumbühl, H. J.: Glacier and lake-level variations in west-central Europe over the last 3500 years, The Holocene, 15(6), 789–801, 2005. 1097

Issar, A. S. and Yakir, D.: Isotopes from wood buried in the Roman siege ramp of Masada: The Roman Period's colder climate, The Biblical Archaeologist, 60(2), 101–106, 1997. 1097

Joerin, U. E., Stocker, T. F., and Schlüchter, C.: Multicentury glacier fluctuations in the Swiss Alps during the Holocene, The Holocene, 16(5), 697–704, 2006. 1097

Jones, P. D.: Climate Variations and Forcing Mechanisms of the Last 2000 Years, in: NATO-ASI Series I, edited by: Bradley, S. and Jouzel, J., Springer-Verlag, Berlin, Germany, 649 pp., 1996. 1090, 1091

Jones, P. D., Briffa, K. R., Barnett, T. P., and Tett, S. F. B.: High-resolution palaeoclimatic records for the last millenium, The Holocene, 8(4), 455–471, 1998. 1090, 1091, 1094, 1095, 1111

Jones, P. D., New, M., Parker, D. E., Martin, S., and Rigor, I. G.: Surface air temperature and its changes over the past 150 years, Rev. Geophys., 37, 173–199, 1999. 1090

Keigwin, L. D.: The Little Ice Age and Medieval Warm Period in the Sargasso Sea, Science, 274(5292), 1504–1508, 1996. 1097, 1113

Krishnaswamy, S., Lal, D., Martin, J. M., and Meybeck, M.: Geochronology of lake sediments, Earth Planet. Sci. Lett., 11, 407–414, 1971. 1091

Luckman, B. H., Briffa, K. R., Jones, P. D., and Schweingruber, F. H.: Tree-ring based reconstruction of summer temperatures at the Columbia Icefield, Alberta, Canada, AD 1073–1983, The Holocene, 7(4), 375–389, 1997. 1090, 1094, 1095, 1096

Mann, M. E., Bradley, R. S., and Hughes, M. H.: Northern Hemisphere temperatures during the past millennium: inferences, uncertainties, and limitations, Geophys. Res. Lett., 26(6), 759–762, 1999. 1090, 1091, 1094, 1095, 1111, 1112

Mann, M. E. and Jones, P. D.: Global Surface Temperatures over the Past Two Millennia,

Geophys. Res. Lett., 30(15), 1820–1823, 2003. 1094
Martínez-Cortizas, A., Pontevedra-Pombal, X., García-Rodeja, E., Nóvoa-Muñoz, J. C., and Shotyk, W.: Mercury in a Spanish peat bog: archive of climate change and atmospheric metal deposition, Science, 284, 939–942, 1999. 1097
Martinson, D. G., Bryan, K., Ghil, M., Hall, M. M., Karl, T. R., Sarachik, E. S., Sorooshian, S., and Talley, L. D. (Eds.): Natural Climate Variability on Decade-to-Century Time Scales, in: National Research Council, National Academy Press, Washington D.C., USA, 630 pp., 1995. 1090, 1091
Naveau, P., Ammann, C., Oh, H. S., and Guo, W.: An automatic statistical methodology to extract pulse like forcing factors in climatic time series: Application to volcanic events, Robock, A. (Ed.), Volcanism and the Earth's Atmosphere, Geophysical Monograph, 139, 177-186, 2003. 1092
National Research Council: Surface Temperature Reconstructions for the Last 2,000 Years, National Academy Press, Washington D.C., USA, 145 pp., 2006. 1090, 1094
Pierre, C.: The oxygen and carbon isotope distribution in the Mediterranean water masses, Mar. Geol., 153, 41–55, 1999. 1098
Plaut, G., Ghil, M., and Vautard, R.: Interannual and interdecadal variability in 335 years of central England temperature, Science, 268, 710–713, 1995. 1090, 1093
Reale, O. and Dirmeyer, P.: Modeling the effects of vegetation on Mediterranean climate during the Roman classical period. Part I: History and model sensitivity, Global Planet. Change, 25, 163–184, 2000. 1098
Reale, O. and Shukla, J.: Modeling the effects of vegetation on Mediterranean climate during the Roman Classical Period: Part II. Model simulation, Global Planet. Change, 25, 185–214, 2000. 1098
Schilman, B., Bar-Matthews, M., Almogi-Labin, A., and Luz, B.: Global climate instability reflected by Eastern Mediterranean marine records during the late Holocene, Palaeogeogr. Palaeoclim. Palaeoecol., 176, 157–176, 2001. 1098
Sicre, M. A., Jacob, J., Ezat, U., Rousse, S., Kissel, C., Yiou, P., Eiriksson, J., Knudsen, K. L., Jansen, E., and Turon, J. L.: Decadal variability of sea surface temperatures off North Iceland over the last 2000 years, Earth Planet. Sci. Lett., 268, 137–142, 2008. 1097
Stommel, H.: Thermohaline convection with two stable regimes of flow, Tellus, 13, 224–230, 1961. 1096
Stuiver, M. and Braziunas, T. F.: Sun, ocean, climate and atmospheric $^{14}CO_2$: an evaluation of

causal and spectral relationship, The Holocene, 3(4), 289–305, 1993. 1096
Taricco, C., Alessio, S., and Vivaldo, G.: Sequence of eruptive events in the Vesuvio area recorded in shallow-water Ionian Sea sediments, Nonlin. Processes Geophys., 15, 25–32, 2008, http://www.nonlin-processes-geophys.net/15/25/2008/. 1092
Tzipermann, E.: Inherently unstable climate behaviour due to weak thermohaline ocean circulation, Nature, 386, 592–595, 1997. 1096
Von Storch, H., Zorita, E., Jones, J. M., Dimitriev, Y., González-Rouco, F., and Tett, S. F. B.: Reconstructing past climate from noisy data, Science, 306, 679–682, 2004. 1091
Vautard, R., Yiou, P., and Ghil, M.: Singular-spectrum analysis: A toolkit for short, noisy chaotic signals, Physica D, 58, 95–126, 1992. 1093, 1094, 1100
Vautard, R. and Ghil, M.: Singular spectrum analysis in nonlinear dynamics, with applications to paleoclimatic time series, Physica D, 35, 395–424, 1989. 1100
White, W. B., Lean, J., Cayan, D. R., and Dettinger, M. D.: A response of global upper ocean temperature to changing solar irradiance, J. Geophys. Res., 102, 3255–3266, 1997. 1096



CPD
4, 1089–1113, 2008

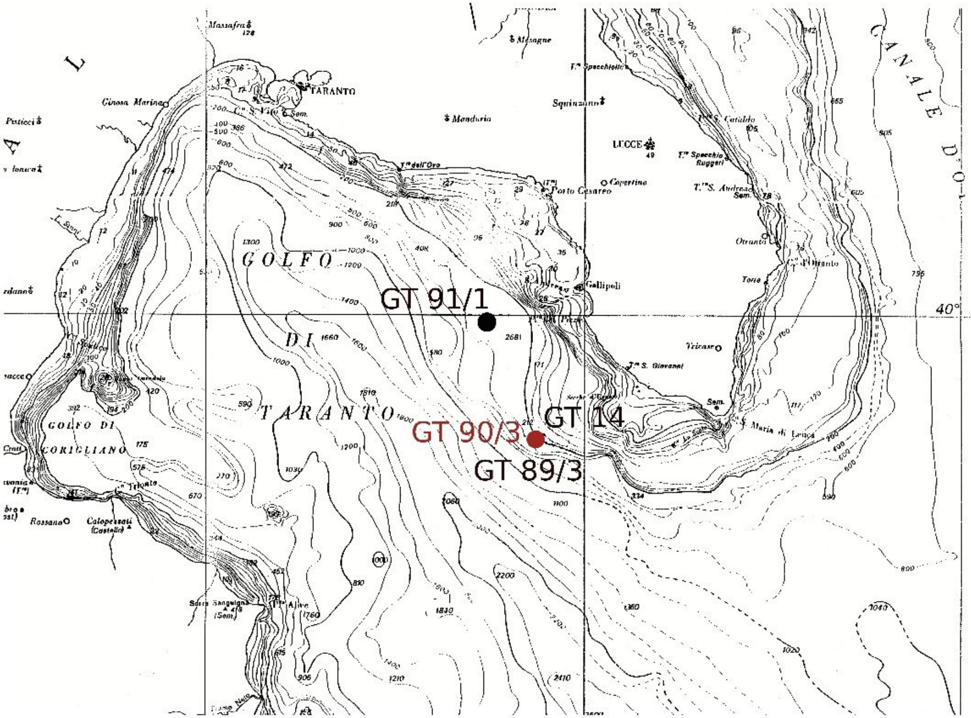


**Fig. 1.** Bathymetric map showing the Gallipoli Terrace in the Gulf of Taranto, Ionian Sea, from which our cores were extracted. We have measured $\delta^{18}O$ in core GT90/3, drilled at (39°45′53″ N, 17°53′33″ E); the core was extracted at a depth of 178 m and has a length of 3.57 m. Cores GT14 and GT89/3 were drilled very close to GT90/3 and are represented by the same point on this map. The Torino cosmogeophysics group measured several profiles in the cores extracted from the Gallipoli Terrace, including $^{210}Pb$ and $^{137}Cs$ activity, as well as pyroxene density (Cini Castagnoli et al., 1990, 1992a; Bonino et al., 1993), $CaCO_3$ content (Cini Castagnoli et al., 1990, 1992a,b), thermoluminescence (Cini Castagnoli et al., 1997, 1998, 1999), and stable isotopes (Cini Castagnoli et al., 1999, 2002b, 2005).

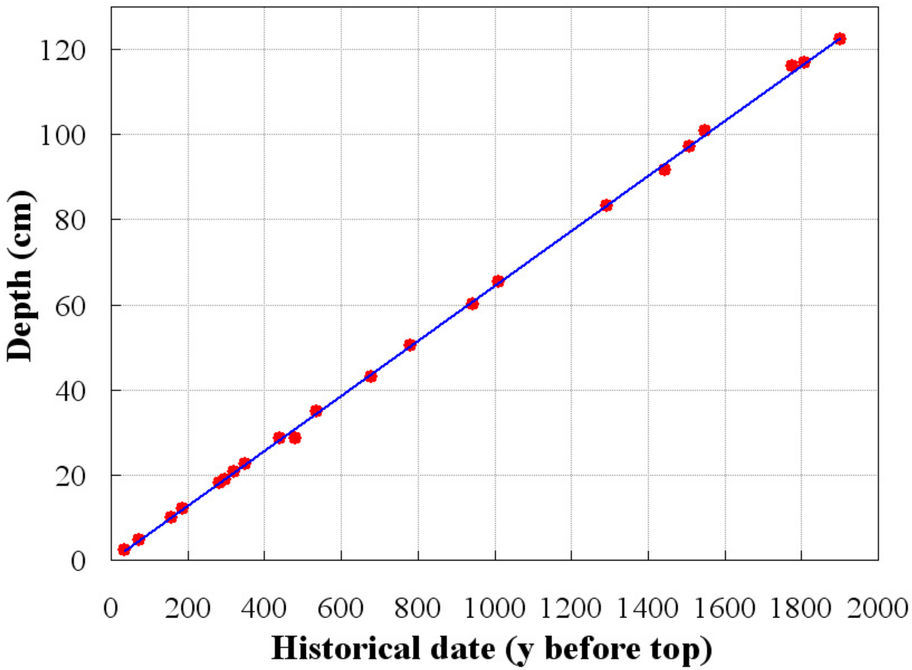


**Fig. 2.** Time-depth relationship. Each point in the figure represents a volcanic eruption, corresponding to a peak in the clinopyroxene time series: 22 historical volcanic eruptions occurred in the Campanian area during the last two millennia and have been identified along the core. The depth at which a volcanic peak is found in the sediment is plotted versus the historical date of the corresponding eruption, expressed in years counted backwards from 1979 AD, i.e. the date of the core top (hence, years-before-top). The straight line resulting from a linear regression fit to the experimental data is also shown. The high correlation coefficient ($r$=0.99) attests to the goodness of the fit.

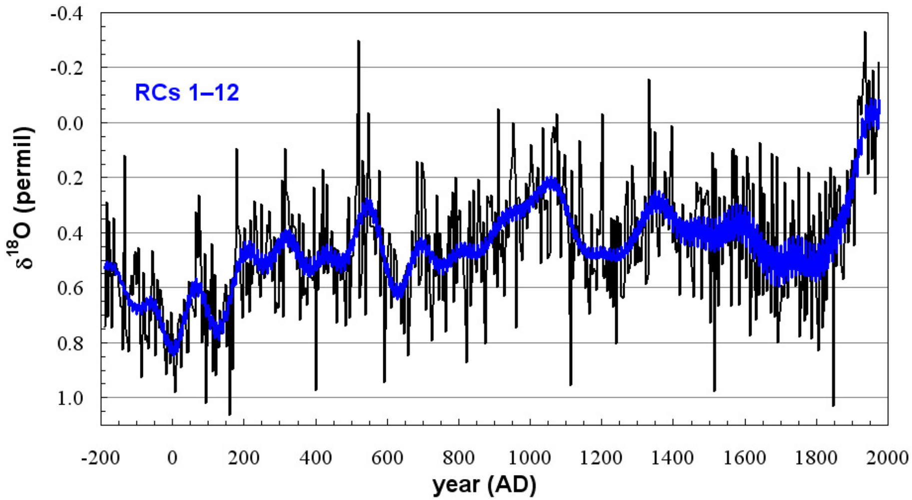


**Fig. 3.** Time series of the oxygen isotope ratio $\delta^{18}O$ measured in the GT90/3 core. Raw data are shown in black solid and the superposed singular-spectrum analysis (SSA) reconstruction (Ghil and Vautard, 1991; Ghil and Taricco, 1997; Ghil et al., 2002) using RCs 1–12 in blue solid; the sampling interval is $\Delta t$=3.87 y, the mean value of the raw data is $x_m$=0.46‰ and their standard deviation is $\sigma_x$=0.23‰.



CPD
4, 1089–1113, 2008



Title Page
Abstract | Introduction
Conclusions | References
Tables | Figures
◂I | ▸I
◂ | ▸
Back | Close
Full Screen / Esc
Printer-friendly Version
Interactive Discussion

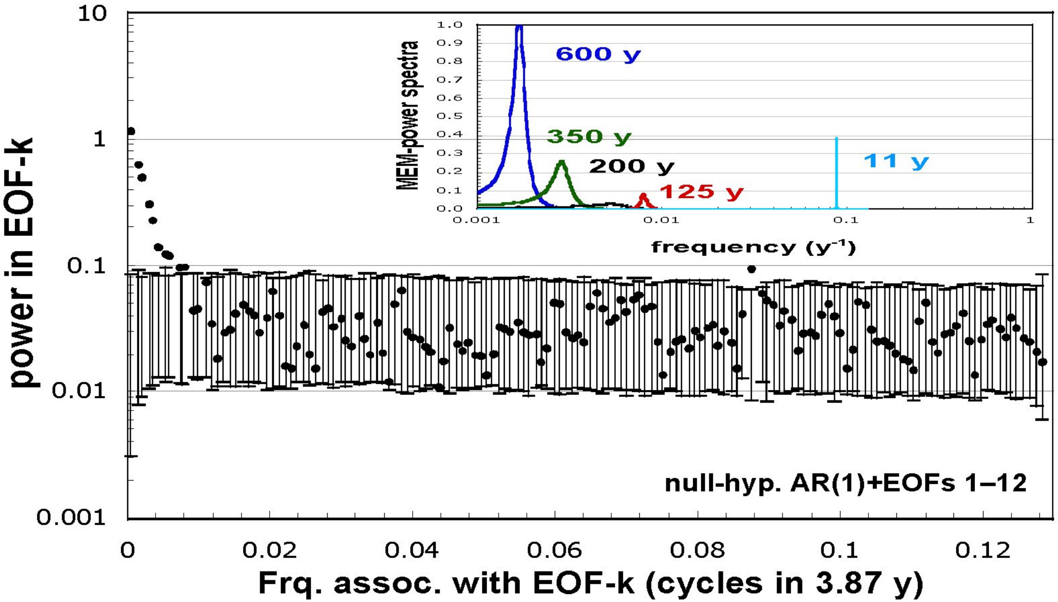


**Fig. 4.** Spectral properties of the $\delta^{18}$O time series in Fig. 3. The main panel shows the Monte Carlo-SSA test (Allen and Smith, 1996). The filled circles indicate the actual eigenvalues of the $\delta^{18}$O record. Inset: individual spectra of the RCs, obtained by the maximum-entropy method (MEM; see http://www.atmos.ucla.edu/tcd/ssa).

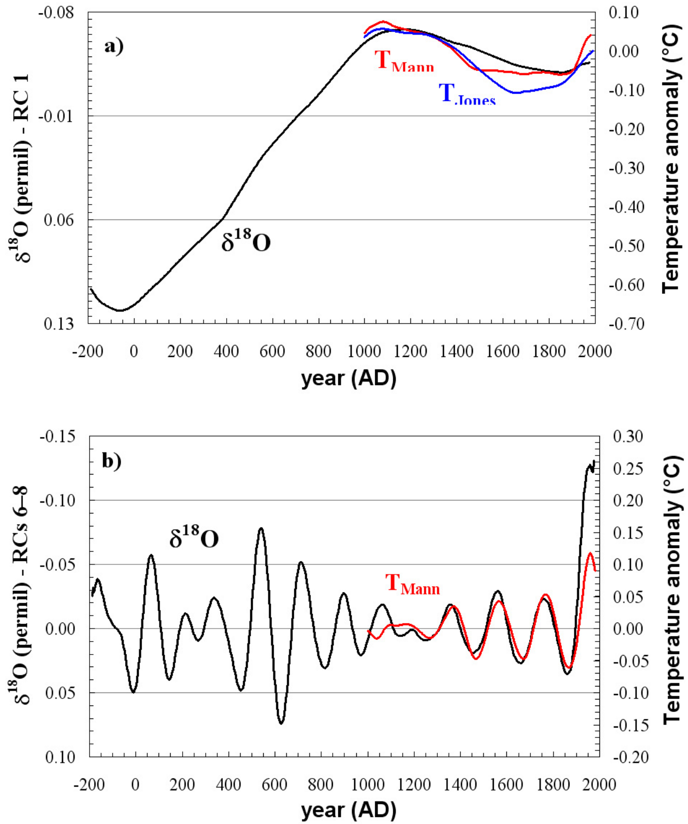


**Fig. 5.** Comparison between the long-term variability in NH temperatures and our $\delta^{18}$O record: **(a)** temperature trend of Mann et al. (1999; RCs 1 and 4 of their data, red), of Jones et al. (1998; RC 1 of their data, blue), and of our $\delta^{18}$O profile (RC 1, inverted; black); **(b)** 200-y temperature oscillation of Mann et al. (1999; RCs 2 and 3 of their data, red) and of our $\delta^{18}$O profile (RCs 6–8, inverted; black).

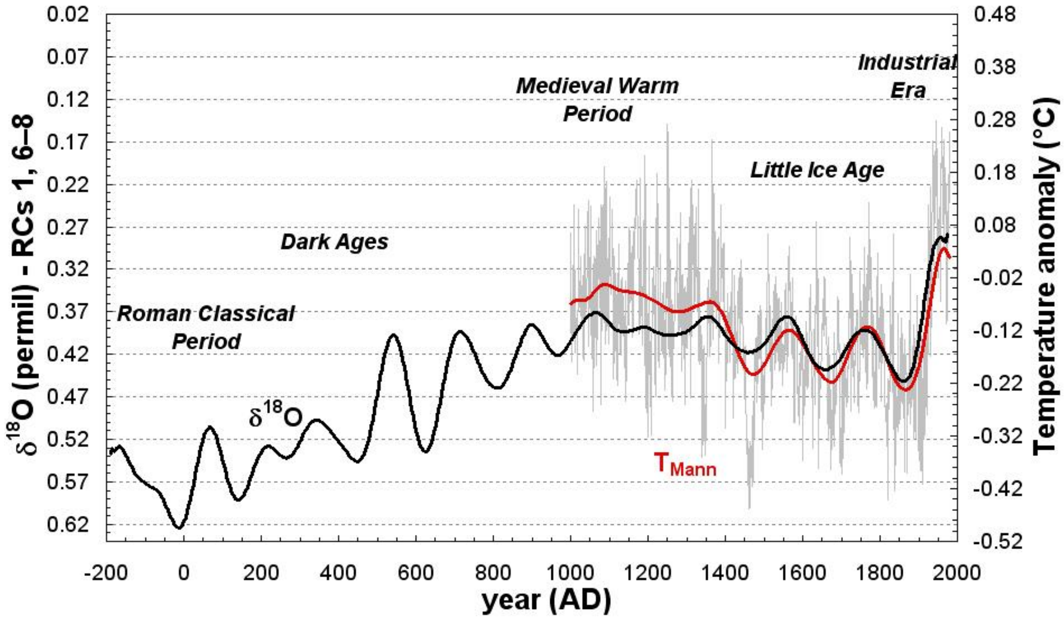


**Fig. 6.** Reconstructed long-term variability of NH temperature (Mann et al., 1999; RCs 1–4, red) and the corresponding $\delta^{18}$O component Σ, given by the sum of the trend and 200-y oscillations (RCs 1 and 6–8, black). The original temperature series of Mann et al. (1999) is also shown (gray) for reference purposes. The match between the $\delta^{18}$O axis (left ordinate) and the temperature anomaly axis (right ordinate) is based on Eq. (1).

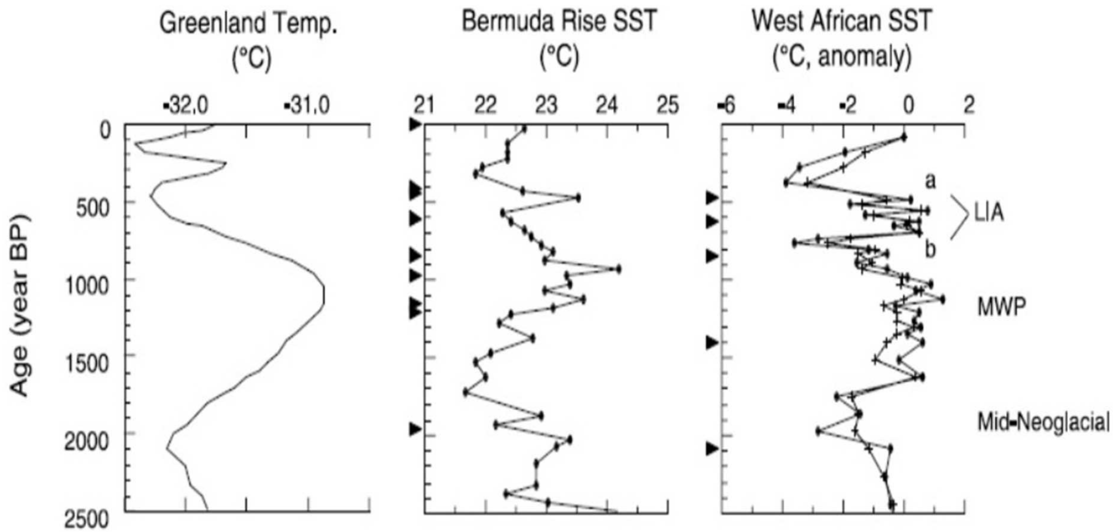


**Fig. 7.** High-resolution records from Greenland ice cores (first panel, Dahl-Jensen et al., 1998), from the western North Atlantic (Bermuda Rise; second panel, Keigwin, 1996), and from the eastern subtropical North Atlantic (DeMenocal et al., 2000, third panel). From DeMenocal, P., Ortiz, J., Guilderson, T., and Sarnthein, M.: Coherent high- and low-latitude climate variability during the Holocene Warm Period, Science, 288, 2198–2202, 2000. Reprinted with permission from AAAS (http://www.sciencemag.org).



CPD
4, 1089–1113, 2008

Two millennia of climate variability

C. Taricco et al.